



Intelligent control method of main road traffic flow based on multi-sensor information fusion

Zhao Deng¹ · Guoming Lu¹

Received: 12 April 2022 / Revised: 1 August 2022 / Accepted: 30 August 2022 / Published online: 25 September 2022
© The Author(s), under exclusive licence to Springer Science+Business Media, LLC, part of Springer Nature 2022

Abstract

In the process of collecting traffic information, traditional traffic flow control methods have some problems, such as high loss rate of sensing and detection information and long average queue length, which lead to the unsatisfactory effect of traffic control and evacuation in main roads. Therefore, based on multi-sensor information fusion technology, this study designs a new intelligent control method of traffic flow on main road. According to the multi-sensor information, the fusion algorithm and measurement equation are designed to obtain the main road traffic sensor position, vehicle linear velocity and other parameters, and update the fusion results in real time. Then, the short-term characteristics of traffic flow are used to control the appearance time of target section. Based on the ordinary differential equation, the main road traffic network is represented by intelligent directed graph, and the intelligent dredging model of urban main road traffic flow is constructed. The simulation results show that in five experimental roads, the average delay time of this method is less than 35 s, the maximum average number of stops is only 8.8, the average queue length is less than 30 m, the average travel speed is more than 25 km/h, the traffic flow per unit time is more than 250veh/10 min, and the traffic congestion index of main road is always more than 5.5. The above indexes of this method are better than those of traditional methods, which verifies that this method has better application performance.

Keywords Multi sensor · Information fusion · Main road traffic · Flow intelligent control

1 Introduction

With the rapid development of urbanization, the traffic pressure of urban trunk road is also increasing, which is followed by the increasing traffic demand of trunk road [1, 2]. An effective solution to alleviate the traffic pressure on urban arterial roads is to realize the active control of arterial road traffic signals, the core of which is to realize the short-term dynamic arterial traffic flow control of the arterial road network [3, 4]. For the main road traffic management, the short-term dynamic traffic flow control can timely and actively allocate the network time and space resources on demand, so as to improve the main road traffic travel efficiency and road network operation stability. For travelers, taking the short-term dynamic main

road traffic flow control as the reference of vehicle path planning can effectively help travelers plan better routes, save time and make travel more convenient. However, due to the complexity and uncertainty of the main road traffic flow, it is difficult to obtain accurate short-term dynamic traffic flow prediction results [5]. Therefore, relevant experts and scholars have carried out research on this and established the related main road traffic flow prediction model. However, most of them do not make full use of the main road traffic flow information except the target road section, and do not fully extract the main road traffic flow transmission characteristic parameters. To some extent, the reliability of prediction results is affected.

At present, the scheduling method of traffic vehicles is mostly accomplished by traffic signal control system [6]. Liu et al. [7] proposed a timing control method. Timing control refers to the control of traffic lights on main roads according to the actual traffic flow on main roads according to the pre-formulated control strategy, so as to complete traffic control. This method can relieve the traffic pressure

✉ Zhao Deng
poil9870@163.com

¹ School of Industrial Design, Hubei University of Technology, Wuhan 430068, China

of main road to a certain extent, but the optimization effect of vehicle delay time and vehicle parking time is poor. Alipour et al. [8] proposed an inductive control method, in which the traffic flow on major roads is detected by detectors. Then, according to the results, adjust the signal parameters, control the traffic flow of each section, to achieve traffic control. This method optimizes the traffic congestion index, but the average driving speed of main roads under this method is still slow, which affects the scheduling of traffic vehicles on urban main roads. Zheng et al. [9] proposed adaptive method control. Adaptive control is to detect changes in traffic flow on main roads in real time, formulate timing schemes, schedule vehicles and predict scheduling effects. Finally, the predicted control effect is compared with the actual traffic flow detection data of the main road, and the control parameters are constantly adjusted to optimize the scheduling strategy. This method can effectively relieve the traffic pressure of the main road, but the control effect is not optimal, and the optimization effect of traffic congestion index, vehicle delay time, vehicle parking time and the average speed of the main road is still not obvious.

Aiming at the above problems, developing a new intelligent traffic flow control method of main road based on the results of multi-sensor information fusion is necessary [10, 11, 12, 13, 14]. Intelligent technologies have been widely developed in different studies [15, 16, 17, 18, 19, 20, 21].

In this method, firstly, the multi-sensor information fusion technology [22, 23, 24, 25] is introduced to control the appearance time of the target partly by using the characteristics of short-time traffic flow. The linear velocity sensor, angular velocity sensor and noise sensor on the main road are used to measure the main parameters of traffic flow control, and the measured information is fused to provide data support for traffic flow control. Considering the flow characteristics at the end of the target segment and the short-term dynamic flow at different times, the data with the greatest similarity in the flow data at different times are selected and matched with the target segment to achieve the purpose of flow control. The traffic flow distribution model of the main roads of intelligent city is constructed to realize the main roads of intelligent traffic flow control. The proposed method can make full use of the main road traffic flow information outside the target section and extract the transmission characteristic parameters of the main road traffic flow, which can guarantee the reliability of the prediction results to a certain extent. The main structure of the method is as follows:

- (a) Set up multiple sensors, design sensor information fusion algorithm and measurement equation, so as to collect the location of traffic sensors on main roads,

vehicle linear speed and other parameters, and complete real-time update and fusion processing of information.

- (b) Control the appearance time of target section according to the short-term characteristics of traffic flow, and establish an ordinary differential equation.
- (c) The intelligent directed graph is used to represent the main road traffic network, and the intelligent dredge model of urban main road traffic flow is constructed.

2 Intelligent control of main road traffic flow

2.1 Multi sensor signal fusion

In order to realize the intelligent control of main road traffic flow, this paper first needs to fuse the multi-sensor signals. Multi sensor information fusion can reduce the loss of single or whole sensor information in detection, and effectively improve the performance of the system composed of multi model sensors. The visual sensing information and the receiving sensing information of the main road traffic are fused. The overall structure of the fusion algorithm is shown in Fig. 1.

In Fig. 1, x and y represent sensor positions, v_x and v_y represent linear velocities of sensors in different directions, θ represents angular displacement, and ω represents angular velocity.

The installation positions of angular velocity sensor, linear velocity sensor and noise sensor are set respectively to generate sensor measured values. Since the detected data has noise, it is necessary to de-noise the data before information fusion. Through theoretical calculation, the covariance of the current state is controlled, and then the information fusion result is obtained by integrating angular velocity sensor, linear velocity sensor and noise sensor.

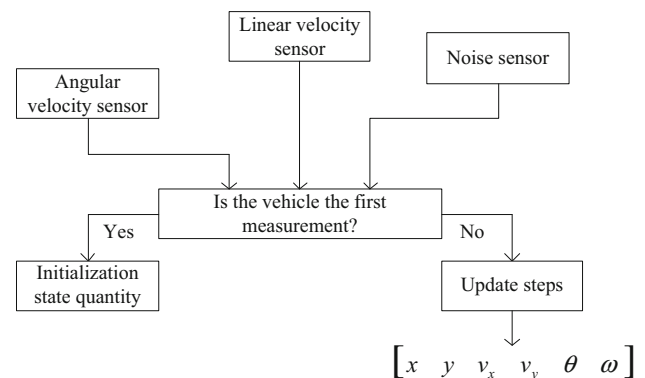


Fig. 1 Overall structure of multi-sensor fusion algorithm in traffic control

Determine whether the vehicle is the first measurement in the result. If so, initialize the state quantity; otherwise, update the steps and repeat the cycle until the judgment result is yes.

The measurement equation of the algorithm is as follows [26]:

$$x_k = f(x_{k-1}) + w_{k-1} \tag{1}$$

In Eq. (1), w_{k-1} is the fusion process noise. Let X represent the system state quantity, which includes the position of each sensor in the main road traffic, the vehicle linear velocity measured by the linear velocity sensor, and the angular velocity measured by the angular velocity sensor, i.e.

$$X = [x \ y \ v_x \ v_y \ \theta \ \omega]^T \tag{2}$$

The observation noise covariance of position, linear velocity and angular velocity can be expressed as follows:

$$R_p = \text{diag}\{1 \times 10^{-2}, 1 \times 10^{-2}\} \tag{3}$$

$$R_v = \text{diag}\{1 \times 10^{-2}, 1 \times 10^{-2}\} \tag{4}$$

$$R_q = \text{diag}\{1 \times 10^{-3}, 1 \times 10^{-4}\} \tag{5}$$

When the first sensor measurement value is generated, the algorithm initializes the state quantity and state covariance, and the initial state quantity and state covariance are obtained as follows:

$$x_0 = [x_0 \ y_0 \ v_{x0} \ v_{y0} \ \theta_0 \ \omega_0] \tag{6}$$

$$Q_0 = \text{diag}\{1 \times 10^{-2}, 1 \times 10^{-2}, 1 \times 10^{-2}, 1 \times 10^{-3}, 1 \times 10^{-4}\} \tag{7}$$

Then, the current sensor state \hat{x}_k is controlled by the state transition matrix, and the expression is as follows:

$$\hat{x}_k = \Phi(k, k - 1)x_{k-1} \tag{8}$$

where, x_{k-1} represents the system state at the previous time, and the state transition matrix $\Phi(k, k - 1)$ can be obtained from the kinematic model as follows:

$$\Phi(k, k - 1) = \begin{bmatrix} 1 & 0 & \cos(\theta)\Delta t & -\sin(\theta)\Delta t & 0 & 0 \\ 0 & 1 & \sin(\theta)\Delta t & \cos(\theta)\Delta t & 0 & 0 \\ 0 & 0 & 1 & 0 & 0 & 0 \\ 0 & 0 & 0 & 1 & 0 & 0 \\ 0 & 0 & 0 & 0 & 1 & \Delta t \\ 0 & 0 & 0 & 0 & 0 & 1 \end{bmatrix} \tag{9}$$

In this formula, Δt represents the sampling interval between the previous time and the current time,

In the Jacobian matrix [27, 28] F can be obtained by the first order Taylor expansion of the state transition function. Using F and Q to complete the control of the current state

covariance \hat{P}_k , the result of multi-sensor traffic information fusion is as follows:

$$\hat{P}_k = FP_{k-1}F^T + Q \tag{10}$$

In Eq. (10), Q is the covariance of noise in the fusion process, which is measured by noise sensor. Q can be expressed as:

$$Q = \text{diag}\{0.6, 1, 6, 2.5, 2.5, 1\} \tag{11}$$

In the process of fusion and update of different kinds of information of multiple sensors. The update gain matrix K is calculated from the observation matrix H [29], the observation noise covariance R and the controlled \hat{P}_k value. Then, the state variable x_k and the state covariance matrix P_k are updated by K , and their expressions are as follows:

$$K = \hat{P}_k H^T (H \hat{P}_k H^T + R) \tag{12}$$

$$x_k = \hat{x}_k + K(z - H\hat{x}_k) \tag{13}$$

$$P_k = (I - KH)\hat{P}_k(I - KH)^T + KRK^T \tag{14}$$

In Eq. (14), the submatrix corresponding to the measured value and state vector in the H matrix is defined as the identity matrix, as follows:

$$H = I_{6 \times 6} \tag{15}$$

According to the above steps, linear velocity sensor, angular velocity sensor and noise sensor are used on the main road. The main parameters of traffic flow control are measured respectively, and the measured information is fused. This process can remove the traditional noise collected by each sensor, so that the obtained information is more accurate, and provide data support for the next flow control.

2.2 Primary flow control based on multi sensor fusion

On the basis of the fusion data obtained above, the flow control of traffic sections is implemented. Due to the short-time dynamic traffic flow delay characteristics between different traffic sections, it is mainly reflected in the distribution delay of traffic flow in the time dimension of main road. The relationship between traffic sections is as follows:

$$f_a(t) = f_b[t + d(t)] \tag{16}$$

In Eq. (16), the change of flow rate of section a with time is described by f_a , that of section b with time is described by f_b , and the function of time delay between section a and section b is described by $d(t)$.

The overall process includes: The traffic section time and the traffic flow at this time are collected, which are divided and reorganized as input data to capture the time

delay characteristics hidden between the short-term flow of the target section and other sections. The continuous sub-sequence with current time and length k is selected as the end time and the flow characteristics of the section at that time to describe the short-term flow of each section at a certain time. The reliability of input data length and similarity was analyzed. On this basis, the length of the sub-sequence is selected, and the shorter sub-sequence has a longer delay range, but the similarity robustness will be weakened by its influence, and the data is easily disturbed by noise. Therefore, only the flow characteristics at the end of the target section P_i (i is the serial number of the section) need to be considered. Get:

$$F_{i,T} = \{f_i(t) | t = T - k - 1, \dots, T\} \tag{17}$$

In Eq. (17), the end time of the input time series is represented by T , and the function of the flow rate of the target section with time is represented by generation $f_i(t)$.

For other sections P_j whose section number is described by j . The data is segmented by traversal delay list, and the short-term dynamic traffic formula at different times is obtained as follows:

$$[F_{i,T-k}, F_{j,1}, \dots, F_{j,T-1}] \tag{18}$$

The similarity measurement matrix between the end time of the target section and the short-term dynamic flow of other sections is described [30].

$$P \in \omega^{(m-1) \times l} \tag{19}$$

In Eq. (19), the total number of sections is described as m , and the number of sub-sequences input from each section is expressed as l . The establishment of the matrix needs to consider the cosine similarity and amplitude similarity. Define the similarity between any two short-term dynamic flow characteristics a and b as:

$$Sim(a, b) = \frac{a \cdot b}{\|a\| \cdot \|b\|} \times \min\left(\frac{\|a\|}{\|b\|}, \frac{\|b\|}{\|a\|}\right) \tag{20}$$

In Eq. (20), Sim is the similarity function [31], $\frac{a \cdot b}{\|a\| \cdot \|b\|}$ and $\min\left(\frac{\|a\|}{\|b\|}, \frac{\|b\|}{\|a\|}\right)$ represent cosine similarity and amplitude similarity respectively.

Select the data with the greatest similarity in the flow data at different times of a certain section, and use it as the best match with the target section to control the best time delay t_{ij}^* between the flow data of the target section and other sections.

$$t_{ij}^* = T - t_j^* \tag{21}$$

$$t_j^* = \arg \max P_{j,t} \tag{22}$$

Among them, the time corresponding to the short-term dynamic flow characteristic with the highest flow

characteristic similarity at the end of the target section in section P_j is represented by t_j^* . The similarity between the flow characteristics at the end of section P_j and the target section and the short-term dynamic flow characteristics at time t . The best match for different sections is described by $P_{j,t}$. Using sigmoid function to normalize the similarity vector, the best similarity vector formula is as follows [32]:

$$V = sigmoid\left(\left\{P_{j,t_j^*} | j \neq i\right\}\right) \tag{23}$$

Through the best matching of energy normalization of different sections, the rationality of the flow control of the target section in the future is guaranteed. Energy gain is defined as [33]:

$$\alpha = \frac{F_{i,T}}{V \times E} \tag{24}$$

Among them, E and F_{j,t_j^*} are the column vectors generated by all elements in the set $\left\{F_{j,t_j^*} | j \neq i\right\}$ and the short-term dynamic flow characteristics of the section P_j at time t_j^* . And E describes the energy of the best matching subsequence between each section and the target section. To control the flow of the target section, it is necessary to normalize the best similarity vector by energy gain energy, and the best similarity vector for completing the energy normalization is:

$$V' = \alpha \times V \tag{25}$$

The preliminary control target section will get:

$$f_i(T + 1) = V' \times \lambda \times \left(f_{j,t_j^*+1} - \sigma\right) \tag{26}$$

Among them, λ represents the column vector generated by all elements in set $\left\{f_{j,t_j^*+1} | j \neq i\right\}$, f_{j,t_j^*+1} represents the flow of section P_j at time $t_j^* + 1$, and σ represents the flow value at the next moment when different sections best match with the target section.

2.3 Traffic flow control model of urban trunk road

After the completion of data fusion and flow control, the method can be used to construct the traffic flow control model of urban trunk roads. Due to the complexity of urban trunk road traffic system, the traffic capacity of each section is different, and the traffic congestion of trunk road will occur. Because the traffic capacity of each section of the intersection is fixed, if it is not cleared in time, when the traffic capacity of the road section is exceeded, congestion will occur.

On the basis of ordinary differential equation, the directed graph $A = (B, O)$ is used to represent the traffic

network of constant trunk road [34], where A is the urban road, $b \in B$ is the section, and $o \in O$ is the intersection point. Set o as the set of input section P_o and output section Q_o , set its cycle time as C_o , and obtain steering flow W_o and loss time L_o through ordinary differential equations, namely:

$$\sum_{o \in P_o} g_{o,i} + L_o = (or \leq) C \tag{27}$$

Use $g_{o,i}$ to indicate that when the main road traffic lines cross, the green light duration of the phase i of the road section O and the full red phase of O under the condition of inequality dense [35] meet the constraints:

$$g_{o,i} \geq \min g_{o,i}, i \in F_o \tag{28}$$

In Eq. (28), $g_{o,i}, \min$ represents that the main road traffic clearing phase allocated by $o \in O$ in phase i has enough available time. Consider the two intersections $O1$ and $O2$ of a section b , as shown in Fig. 1 and Fig. 2. Combined with ordinary differential equation control, the conservation function of arterial road traffic section b can be obtained [36]:

$$xb(k + 1) = xb(k) + T[qb(k) - sb(k) + db(k) - ub(k)] \tag{29}$$

where $xb(k)$ is the flow of section b at time period KT . $qb(k)$ and $ub(k)$ are road sections b and $[KT, (k + 1)T]$ is the flow of entering and leaving. T is the dredging time, let the dredging flow be $sb(k) = tb, 0qb$, the departure rate is $t(b, 0)$, and the degree of road section density is restricted by:

$$0 \leq xb(k) \leq xb, \max, \forall b \in B \tag{30}$$

In Eq. (30), xb, \max is the maximum density, which can protect the dredging area. Denote the inflow of road section b as $qb(k) = \sum \omega \in I0tw, bu\omega(k), tw, b$, and follow the principle of simplification of dredging to obtain a linear multivariable feedback function [37]:

$$g(k) = g^N - F(k) \tag{31}$$

In Eq. (31), F is the solution of algebraic differential equation, and g^N is the required grooming variable. Therefore, if the traffic flow length $L(k)$ of the main road is

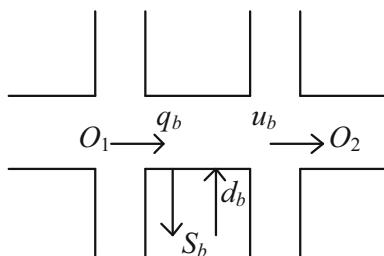


Fig. 2 Urban main road traffic road

used to adjust g^N in real time, the main road traffic flow $xb(k)$ can be measured by installing a coil detection in the middle of the road. At the same time, in order to meet the constraint conditions of ordinary differential equation, the green light duration is set as $g_{o,i}$, and the main road traffic flow dredging model is as follows:

$$\phi(\tilde{g}_{o,i}) = \frac{1}{2} \sum i \in F_o (\tilde{g}_{o,i} - g_{o,i})^2 / g_{o,i} \tag{32}$$

The calculated green light correction time is $\tilde{g}_{o,i}$ and n . When Eq. (32) satisfies the constraint condition, the number of iterations is the same as the total number of variables associated with the grooming configuration, usually 3 to 4 times. The schematic diagram of the urban arterial road traffic is shown in Fig. 2, and the simplified model of the arterial road traffic flow is shown in Fig. 3.

A stable point of optimal grooming can be obtained through the above. When the grooming model reaches a stable state, the green light duration is not considered, and each state on the urban arterial traffic route can be measured with any value between 0 and 1. It not only represents the density of traffic flow on the main road in a certain period of time, but also represents that the sum of the state measures of all States on each route at any time is 1. Therefore, the grooming model established in this study can be used to change the rate of change of signal lights to alleviate the problem of urban main road traffic jams.

3 Simulation experiment and analysis

To validate the design based on multi-sensor information fusion of the main road traffic intelligent control method is effective and feasible, structures, simulation platform, the selection of evaluation parameters, including the main road traffic congestion index, the average vehicle delay time, average vehicle parking times average travel speed, road, etc., analysis and compare the method and effect of three kinds of traditional methods of scheduling [38, 39, 40, 41, 42].

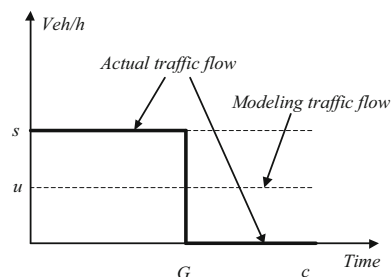


Fig. 3 Simplified model of main road traffic flow

3.1 Overview of experimental environment

The road network in a central urban area of a certain city is selected as the real-time environment of this experiment. In this area, two vertical, three horizontal and five roads intersect to form a main road traffic network, and a total of 24 signal control systems are set up at the control intersection. The simulation diagram of the main road traffic network is shown in Fig. 4.

The initial parameter settings and the current congestion situation of the arterial road traffic network are shown in Tables 1 and 2.

3.2 Simulation platform

The simulation experiment is carried out on VISSIM simulation platform. The VISSIM simulation platform is an effective modeling tool specially used to evaluate arterial road traffic engineering design and urban planning schemes. Its structural model is shown in Fig. 5.

The basic structure of VISSIM simulation platform consists of two parts: Main road traffic flow simulation module and traffic control module. Among them, the former function is to simulate the main road traffic operation, the latter function is according to the simulation collaborative scheduling operation program.

3.3 Test indicators

In order to better reflect the performance of each traffic control method (this paper scheduling method, timing control scheduling method, induction control scheduling method and adaptive control scheduling method). This paper takes the average delay time of vehicles, average parking times, vehicle flow per unit time, average queue length and average travel speed of each trunk road as evaluation indexes, and then carries out weighted

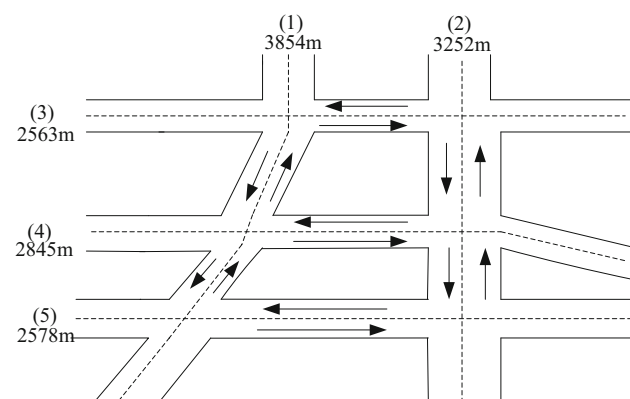


Fig. 4 Simulation diagram of main road traffic network in a certain area of a city

Table 1 Initial parameter setting of main road traffic network

Experimental parameters	Parameter value
Road Network	6 intersections, 5 arterial roads
Vehicle entry rate	0.35veh/s
Vehicle departure rate	1.50 veh/s
Average parking space	0.35 m
sampling period	3 min

quantitative calculation to obtain congestion index, which is used to evaluate the scheduling performance of the method. The calculation formula is as follows:

$$T(P) = w_1A + w_2B + w_3C + w_4D + w_5E \quad (33)$$

In the Eq. (33), $T(P)$ is the congestion index; w_1, w_2, w_3, w_4 and w_5 were all weighted factors; A is the average delay time of vehicles; B is the average number of vehicles stopping; C is the average queue length; D is the average travel speed; E is the traffic flow per unit time.

3.4 Test result

3.4.1 Performance of traffic control method in this paper

By comparing the performance evaluation results obtained in Table 3 with the congestion results investigated in Table 2 before using the method in this paper, it can be seen that in the five selected roads, the average delay time under the method in this paper is significantly shorter than the original congestion situation, indicating that the method in this paper can effectively improve the index of average delay time. The results of all indicators under Road no. 3 are poor, indicating that the effect of the proposed method on road No. 3 is not good. The method of average parking time and average queue length in other road has played a certain effect, the average speed increased, the sons of thunder flow per unit time is also greatly increased, the index of major road traffic congestion has decreased, the main road traffic congestion degree eased, illustrates the method practical application effect is better.

3.4.2 Performance of timing control method proposed in reference Liu et al. [7]

Table 4 shows the performance evaluation results of the timing control scheduling method. The results are compared with the results of the proposed method in Table 3. The analysis shows that the timing control scheduling method performs better than the proposed method on Road 3, but its values are not as good as the results obtained by the proposed method on other roads. It shows that the

Table 2 Congestion survey results

Main road traffic	1	2	3	4	5
Average delay time (s)	36	45	30	58	47
Average parking times (time)	8.4	10.3	7.2	13.4	11.2
Average queue length (m)	26	32	22	43	35
Average travel speed (km/h)	25.6	15.3	32.0	10.8	14.2
Traffic flow per unit time (veh/10 min)	245	224	265	187	230
Traffic congestion index of main roads	5.47	8.65	3.32	9.67	7.69
Traffic congestion degree of main roads	Mild congestion	Moderate congestion	Basically smooth	Heavy congestion	Moderate congestion

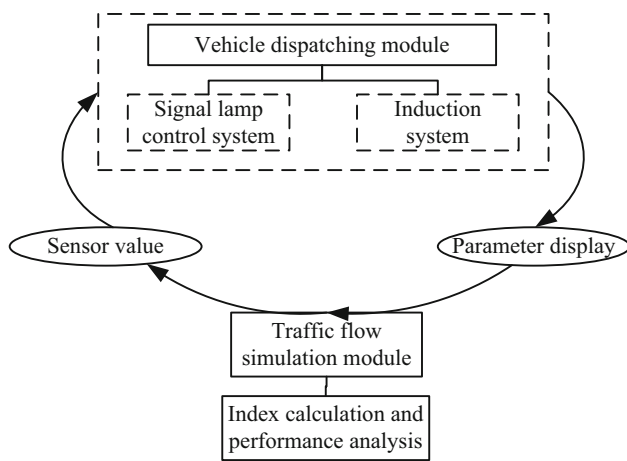


Fig. 5 Structure model of VISSIM simulation platform

method in this paper is more effective in practical application on other roads except road no. 3.

3.4.3 Performance of induction control method proposed in Alipour et al. [8]

According to the performance evaluation results in Table 5, it can be seen that the induction control scheduling method has a better effect on the traffic flow control of main road no. 1 and No. 4, which is superior to the results of the

proposed method and the timing control scheduling method.

3.4.4 Performance of adaptive control method proposed in Zhang et al. (2020)

As can be seen from Table 6, the application effect of the adaptive control scheduling method is poor compared with other methods under the five selected roads, and the actual application performance is low.

As shown in Table 3 to Table. 6, under the proposed method, the average delay time of the five roads is 35.8 s, which is 7.4 s less than before the proposed method. The average stop time is 8.74 s, which is 1.36 s less than before the application of the method in this paper. The average queue length is 28.2 s, which is 3.4 s less than before. The average driving speed is 23.86 km/h, which is 4.28 km/h higher than before. The lightning flux per unit time is 247.4 times /10 min, which is 17.2 times /10 min higher than before the application of the method in this paper. The traffic congestion index of main roads is 6.008, which is 0.952 lower than before the application of the method in this paper. Traffic congestion on major roads has also eased. The results obtained from the above indicators all show that the performance of the proposed method is good. The traffic congestion degree of the main roads of the five

Table 3 Performance evaluation results of traffic control methods in this paper

Main road traffic	1	2	3	4	5
Average delay time (s)	32	33	35	35	34
Average parking times (time)	7.6	7.5	8.6	8.8	8.0
Average queue length (m)	22	25	30	21	24
Average travel speed (km/h)	25.8	26.1	23.3	27.8	26.3
Traffic flow per unit time (veh/10 min)	250	242	258	235	252
Traffic congestion index of main roads	5.25	5.45	5.32	5.21	5.44
Traffic congestion degree of main roads	Mild congestion	Mild congestion	Mild congestion	Mild congestion	Mild congestion

Table 4 Performance evaluation results of timing control scheduling method

Main road traffic	1	2	3	4	5
Average delay time (s)	38	44	33	45	47
Average parking times (time)	8.8	11.1	7.0	12.2	11.2
Average queue length (m)	25	33	25	35	33
Average travel speed (km/h)	24.4	15.5	22.7	16.4	16.6
Traffic flow per unit time (veh/10 min)	243	222	255	220	232
Traffic congestion index of main roads	5.44	8.54	5.21	9.67	7.45
Traffic congestion degree of main roads	Mild congestion	Moderate congestion	Mild congestion	Moderate congestion	Moderate congestion

Table 5 Performance evaluation results of induction control scheduling method

Main road traffic	1	2	3	4	5
Average delay time (s)	28	60	45	30	49
Average parking times (time)	6.8	12.8	12.5	7.8	13.5
Average queue length (m)	20	40	33	25	36
Average travel speed (km/h)	35.5	11.4	14.4	33.2	15.6
Traffic flow per unit time (veh/10 min)	264	188	236	257	233
Traffic congestion index of main roads	5.44	9.48	7.92	8.96	7.84
Traffic congestion degree of main roads	Basically smooth	Heavy congestion	Moderate congestion	Basically smooth	Moderate congestion

Table 6 Performance evaluation results of adaptive control scheduling method

Main road traffic	1	2	3	4	5
Average delay time (s)	44	45	46	50	46
Average parking times (time)	12.7	13.6	14.2	13.4	12.1
Average queue length (m)	33	32	36	35	37
Average travel speed (km/h)	15.5	13.9	15.2	16.1	16.6
Traffic flow per unit time (veh/10 min)	230	227	238	220	233
Traffic congestion index of main roads	7.36	8.12	7.66	7.90	7.77
Traffic congestion degree of main roads	Moderate congestion	Moderate congestion	Moderate congestion	Moderate congestion	Moderate congestion

main roads is effectively balanced after the scheduling method in this paper, and the traffic congestion level of the moderate and severe trunk roads is reduced. Compared with the other three scheduling methods, it can be seen that under the operation of this method, the traffic condition of the main road in the central area of the city has been significantly improved. Therefore, the performance of the collaborative scheduling method is better.

4 Conclusion

In order to solve the problems of long average delay time, long average queue length and slow average travel speed in traditional traffic flow control methods, an intelligent traffic flow control method based on multi-sensor information fusion is proposed in this paper. The final results show that the test data of average delay time, average stop times, average queue length, average driving speed, traffic flow per unit time and traffic congestion index of main road are

all satisfactory, which proves that the proposed method has good application performance. The reason to achieve such a result is that this paper fuses the signals of multiple sensors and de-noises the results to ensure the accuracy of the sensor signal. On this basis, flow control is carried out to achieve better modeling. However, due to the limited time and technology, the rate of multi-sensor signal fusion in this paper is low and still needs to be improved. In the future, this paper will conduct more in-depth research on this problem, so as to improve the research content of this paper, realize the intelligent control of traffic flow of main road, and make contributions to the practical application.

Author contributions These authors contributed equally to this work.

Funding Not applicable.

Data availability All data are available from the corresponding author.

Declarations

Conflict of interest The authors declare that they have no known competing financial interests or personal relationships that could have appeared to influence the work reported in this paper.

Ethical approval Not applicable.

Consent to participate Not applicable.

Consent for publication Not applicable.

References

- Chen, J., Wang, Q., Huang, J., Chen, X.: Motorcycle ban and traffic safety: evidence from a quasi-experiment at Zhejiang China. *J Adv Transport*. **2021**, 1–13 (2021)
- Chen, S., Zhang, J., Meng, F., Wang, D., Wei, Z., Zhang, W.: A Markov chain position prediction model based on multidimensional correction. *Complexity* (2021). <https://doi.org/10.1155/2021/6677132>
- Luo, G., Zhang, H., Yuan, Q., Li, J., Wang, F.: ESTNet: Embedded spatial-temporal network for modeling traffic flow dynamics. *IEEE Trans. Intell. Transp. Syst.* (2022). <https://doi.org/10.1109/TITS.2022.3167019>
- Zhao, C., Liao, F., Li, X., Du, Y.: Macroscopic modeling and dynamic control of on-street cruising-for-parking of autonomous vehicles in a multi-region urban road network. *Transp. Res.* **128**, 103176 (2021). <https://doi.org/10.1016/j.trc.2021.103176>
- Frejo, J.R.D., Schutter, B.D.: Logic-based traffic flow control for ramp metering and variable speed limits-part 1: Controller. *IEEE Trans. Intell. Transp. Syst.* **15**(9), 1–11 (2020)
- Gong, X., Wang, L., Mou, Y., Wang, H., Wei, X., Zheng, W., Yin, L.: Improved Four-channel PBTDP control strategy using force feedback bilateral teleoperation system. *Int. J. Control* **20**(3), 1002–1017 (2022). <https://doi.org/10.1007/s12555-021-0096-y>
- Liu, T., Abouzeid, A.A., Julius, A.A.: Traffic flow control in vehicular multi-hop networks with data caching and infrastructure support. *IEEE/ACM Trans. Networking* **28**(1), 1–11 (2020)
- Alipour, A., Kebriaei, H., Ramezani, M.: Analytical optimal solution of perimeter traffic flow control based on MFD dynamics: A pontryagin's maximum principle approach. *IEEE Trans. Intell. Transp. Syst.* **20**(9), 3224–3234 (2019)
- Zheng, Y., Wang, J., Li, K.: Smoothing traffic flow via control of autonomous vehicles. *IEEE Internet Things J.* **7**(5), 3882–3896 (2020)
- Wang, Y., Han, X., Jin, S. MAP based modeling method and performance study of a task offloading scheme with time-correlated traffic and VM repair in MEC systems. *Wireless Networks*. (2022). <https://doi.org/10.1007/s11276-022-03099-2>
- Zou, W., Sun, Y., Zhou, Y., Lu, Q., Nie, Y., Sun, T., Peng, L. Limited sensing and deep data mining: A new exploration of developing city-wide parking guidance systems. *IEEE Intelligent Transportation Systems Magazine* **14**(1) 198–215 9052749 <https://doi.org/10.1109/TITS.2020.2970185>
- Fang, Y., Min, H., Wu, X., Wang, W., Zhao, X., Mao, G.: On-Ramp merging strategies of connected and automated vehicles considering communication delay. *IEEE Transactions on Intelligent Transportation Systems* **23**(9), 15298–15312 (2022). <https://doi.org/10.1109/TITS.2022.3140219>
- Wu, H., Jin, S., Yue, W. Pricing policy for a dynamic spectrum allocation scheme with batch requests and impatient packets in cognitive radio networks. *Journal of Systems Science and Systems Engineering* **31**(2), 133–149 (2022). <https://doi.org/10.1007/s11518-022-5521-0>
- Meng, F., Xiao, X., Wang, J.: Rating the crisis of online public opinion using a multi-level index system. *The International Arab Journal of Information Technology* **19**(4), 597–608 (2022). <https://doi.org/10.34028/iajit/19/4/4>
- Cao, B., Zhang, W., Wang, X., Zhao, J., Gu, Y., Zhang, Y.: A memetic algorithm based on two_Arch2 for multi-depot heterogeneous-vehicle capacitated arc routing problem. *Swarm Evol. Comput.* **63**, 100864 (2021). <https://doi.org/10.1016/j.swevo.2021.100864>
- Lv, Z., Li, Y., Feng, H., Lv, H.: Deep learning for security in digital twins of cooperative intelligent transportation systems. *IEEE Transact. Intell. Transport. Syst.* (2021). <https://doi.org/10.1109/TITS.2021.3113779>
- Han, Y., Wang, B., Guan, T., Tian, D., Yang, G., Wei, W., Chuah, J. H. Research on Road Environmental Sense Method of Intelligent Vehicle Based on Tracking Check. *IEEE transactions on intelligent transportation systems*, (2022). <https://doi.org/10.1109/TITS.2022.3183893>
- Wang, J., Tian, J., Zhang, X., Yang, B., Liu, S., Yin, L., Zheng, W.: Control of time delay force feedback teleoperation system with finite time convergence. *Front. Neurobot.* (2022). <https://doi.org/10.3389/fbot.2022.877069>
- Xu, Y.P., Ouyang, P., Xing, S.M., Qi, L.Y., et al.: Optimal structure design of a PV/FC HRES using amended Water Strider Algorithm. *Energy Rep.* **7**, 2057–2067 (2021)
- Ma, Z., Zheng, W., Chen, X., Yin, L.: Joint embedding VQA model based on dynamic word vector. *PeerJ Computer Science* **7**, e353 (2021). <https://doi.org/10.7717/peerj-cs.353>
- Chen, P., Pei, J., Lu, W., Li, M. A deep reinforcement learning based method for real-time path planning and dynamic obstacle avoidance. *Neurocomputing*, 497, 64–75. (2022). <https://doi.org/10.1016/j.neucom.2022.05.006>
- Sui, T., Marelli, D., Sun, X., Fu, M.: Multi-sensor state estimation over lossy channels using coded measurements. *Automatica* **111**, 108561 (2020). <https://doi.org/10.1016/j.automatica.2019.108561>
- Du Y, Qin B, Zhao C, Zhu Y, Cao J, Ji Y.: A novel spatio-temporal synchronization method of roadside asynchronous

- MMW radar-camera for sensor fusion. *IEEE transactions on intelligent transportation systems*, (2021)
24. Lv, Z., Chen, D., Feng, H., Wei, W., Lv, H.: Artificial intelligence in underwater digital twins sensor networks. *ACM Transact Sensor Net* **18**(3), 27 (2022). <https://doi.org/10.1145/3519301>
 25. Sun, Q., Lin, K., Si, C., Xu, Y., Li, S., Gope, P.: A Secure and Anonymous Communicate Scheme over the Internet of Things. *ACM Transactions on Sensor Networks*. (2022). <https://doi.org/10.1145/3508392>
 26. Wang, Y.Z., Yang, X.G., Liang, H.L., Liu, Y.D.: A Review of the self-adaptive traffic signal control system based on future traffic environment. *J. Adv. Transp.* **10**(3), 1–12 (2018)
 27. Li, D., Zhao, X., Cao, P.: An enhanced motorway control system for mixed manual/automated traffic flow. *IEEE Syst. J.* **22**(99), 1–9 (2020)
 28. Li, Z., Chen, L., Nie, L., Yang, S.X.: A novel learning model of driver fatigue features representation for steering wheel angle. *IEEE Transactions on Vehicular Rechnology* **71**(1), 269–281 (2022)
 29. Fernandez FG, Li Z.: Integrated control of traffic flow [PH.D. and M.PHIL. theses abstracts], *IEEE Intelligent Transportation Systems Magazine*, 12(3), 157–159. (2020)
 30. Tettamanti, T., Torok, A., Varga, I.: Dynamic road pricing for optimal traffic flow management by using nonlinear model predictive control. *IET Intel. Transport Syst.* **13**(7), 1139–1147 (2019)
 31. Yan, R., Yang, D., Wijaya, B., Yu, C.: Feedforward compensation-based finite-time traffic flow controller for intelligent connected vehicle subject to sudden velocity changes of leading vehicle. *IEEE Trans. Intell. Transp. Syst.* **21**(8), 3357–3365 (2020)
 32. Wang, Y.Q., Zhou, C.F., Wang, J.W., Ni, X.P.: Evolvement laws and stability analyses of traffic network constituted by changing ramps and main road. *Int. J. Mod. Phys. B* **33**(20), 23–24 (2019)
 33. Han, L., Huang, Y.S.: Short-term traffic flow prediction of road network based on deep learning. *IET Intel. Transport Syst.* **14**(6), 495–503 (2020)
 34. Novikov, A., Zyryanov, V., Feofilova, A.: Dynamic traffic re-routing as a method of reducing the congestion level of road network elements. *Istrazivanja i Projektovanja za Privredu* **16**(1), 70–74 (2018)
 35. Rodger, J.A.: Advances in multisensor information fusion: A Markov-Kalman viscosity fuzzy statistical predictor for analysis of oxygen flow, diffusion, speed, temperature, and time metrics in CPAP. *Expert. Syst.* **35**(4), 1–21 (2018)
 36. Chang, Y.T., Sun, L.F., Pu, J.X.: Air target identification using multiple sensors based on modified evidence support. *Comput. Simulat.* **37**(7), 394–398 (2020)
 37. Jin, Y.L., Jia, Z., Wang, P., Sun, Z.: Quantitative assessment on truck-related road risk for the safety control via truck flow estimation of various types. *IEEE Access* **7**, 88799–88810 (2019)
 38. Niu, Z., Zhang, B., Dai, B., Zhang, J., Shen, F., Hu, Y., Fan, Y., Zhang, Y.: 220 GHz multi circuit integrated front end based on solid-state circuits for high speed communication system. *Chin. J. Electron.* **31**(3), 569–580 (2022). <https://doi.org/10.1049/cje.2021.00.295>
 39. Yan, A., Fan, Z., Ding, L., Cui, J., Huang, Z., Wang, Q., Wen, X.: Cost-effective and highly reliable circuit components design for safety-critical applications. *IEEE Transact. Aerospace Electronic Syst.* (2021). <https://doi.org/10.1109/TAES.2021.3103586>
 40. Liu, C., Wu, D., Li, Y., Du, Y.: Large-scale pavement roughness measurements with vehicle crowdsourced data using semi-supervised learning. *Transport Res* **125**, 103048 (2021). <https://doi.org/10.1016/j.trc.2021.103048>
 41. Liu, H., Shi, Z., Li, J., Liu, C., Meng, X., Du, Y., Chen, J.: Detection of road cavities in urban cities by 3D ground-penetrating radar. *Geophysics* **86**(3), A25–A33 (2021)
 42. Ma, X., Quan, W., Dong, Z., Dong, Y., Si, C.: Dynamic response analysis of vehicle and asphalt pavement coupled system with the excitation of road surface unevenness. *Appl. Math. Model.* **104**, 421–438 (2022). <https://doi.org/10.1016/j.apm.2021.12.005>

Publisher's Note Springer Nature remains neutral with regard to jurisdictional claims in published maps and institutional affiliations.

Springer Nature or its licensor holds exclusive rights to this article under a publishing agreement with the author(s) or other rightsholder(s); author self-archiving of the accepted manuscript version of this article is solely governed by the terms of such publishing agreement and applicable law.



projects at the same time.

Zhao Deng born in September 1981, associate professor. He received a bachelor's degree in product design from Hubei University of Technology in 2003. In 2008, he graduated from Hubei University of Technology majoring in product design with a master's degree. Now working in Hubei University of Technology. His research fields include: product design, travel and transportation design. Published 12 academic papers and participated in five research



Guoming Lu male, born in May 1992, and he is a graduate student. He received a bachelor's degree in product design from Hubei University of Technology in 2018. Now studying at Hubei University of Technology. His research areas include: sustainable intelligent transportation design.